5560 *Inorg. Chem.* **2010**, *49*, 5560–5572
DOI: 10.1021/ic100386c

Inorganic Chemistry
Article

NH NMR Shifts of New Structurally Characterized *fac*-$[Re(CO)_3(polyamine)]^{n+}$ Complexes Probed via Outer-Sphere Hydrogen-Bonding Interactions to Anions, Including the Paramagnetic $[Re^{IV}Br_6]^{2-}$ Anion

Theshini Perera, Patricia A. Marzilli, Frank R. Fronczek, and Luigi G. Marzilli*

Department of Chemistry, Louisiana State University, Baton Rouge, Louisiana 70803

Received February 25, 2010

fac-$[Re^{I}(CO)_3L]^n$ complexes serve as models for short-lived *fac*-$[^{99m}Tc^{I}(CO)_3L]^n$ imaging tracers (L = tridentate ligands forming two five-membered chelate rings defining the L face). Dangling groups on L, needed to achieve desirable biodistribution, complicate the NMR spectra, which are not readily understood. Using less complicated L, we found that NH groups (*exo*-NH) projecting toward the L face sometimes showed an upfield shift attributable to steric shielding of the *exo*-NH group from the solvent by the chelate rings. Our goal is to advance our ability to relate these spectral features to structure and solution properties. To investigate whether *exo*-NH groups in six-membered rings exhibit the same effect and whether the presence of dangling groups alters the effect, we prepared new *fac*-$[Re(CO)_3L]^{n+}$ complexes that allow direct comparisons of *exo*-NH shifts for six-membered versus five-membered chelate rings. New complexes were structurally characterized with the following L: dipn [*N*-3-(aminopropyl)-1,3-propanediamine], *N*′-Medipn (3,3′-diamino-*N*-methyldipropylamine), *N*,*N*-Me_2dipn (*N*,*N*-dimethyldipropylenetriamine), aepn [*N*-2-(aminoethyl)-1,3-propanediamine], trpn [tris-(3-aminopropyl)amine], and tren [tris-(2-aminoethyl)amine]. In DMSO-d_6, the upfield *exo*-NH signals were exhibited by all complexes, indicating that the rings sterically shield the *exo*-NH groups from bulky solvent molecules. This interpretation was supported by *exo*-NH signal shift changes caused by added halide and $[ReBr_6]^{2-}$ anions, consistent with outer-sphere hydrogen-bond interactions between these anions and the *exo*-NH groups. For *fac*-$[Re(CO)_3(dipn)]PF_6$ in acetonitrile-d_3, the *exo*-NH signal shifted further downfield in the series, $Cl^- > Br^- > I^-$, and the plateau in the shift change required a lower concentration for smaller anions. These results are consistent with steric shielding of the *exo*-NH groups by the chelate rings. Nevertheless, despite its size, the shape and charge of $[ReBr_6]^{2-}$ allowed the dianion to induce large upfield paramagnetic shifts of the *exo*-NH signal of *fac*-$[Re(CO)_3(dipn)]PF_6$. This dianion shows promise as an outer-sphere hydrogen-bonding paramagnetic shift reagent.

Introduction

fac-$[Re(CO)_3L]^n$ complexes have provided a good model system for interpreting the nature of the analogous *fac*-$[^{99m}Tc(CO)_3L]^n$ imaging agents formed in tracer level preparations.[1,2] The convenient generation of the *fac*-$[^{99m}Tc(CO)_3(H_2O)_3]^+$ precursor[3,4] and the straightforward preparation of the *fac*-$[Re(CO)_3(H_2O)_3]^+$ precursor[5] have contributed toward the development of new *fac*-$[^{99m}Tc(CO)_3L]^n$ radiopharmaceuticals because *fac*-$[Re(CO)_3(H_2O)_3]^+$ allows simulation of the synthesis of ^{99m}Tc complexes in aqueous media.[2] Recently, Re complexes have been emerging as radiopharmaceuticals in their own right, owing to the possibility of utilizing the $\{^{186/188}Re(CO)_3\}^+$ core for therapeutic purposes.[6,7] Additional evidence of the growing importance of this field is found in a recent report of a rapid and versatile microwave synthesis for the preparation of chelate complexes with the *fac*-$\{M^{I}(CO)_3\}^+$ core (M = ^{99m}Tc, Re).[8]

fac-$[^{99m}Tc(CO)_3L]^n$ complexes bearing tridentate ligands (L) are rather robust,[6,9] and tridentate ligand systems bearing a dangling group with functional groups for conjugation to biomolecules or for directing the agent to a particular target

*To whom correspondence should be addressed. E-mail: lmarzil@lsu.edu.

(1) He, H.; Lipowska, M.; Xu, X.; Taylor, A. T.; Marzilli, L. G. *Inorg. Chem.* **2007**, *46*, 3385–3394.
(2) He, H. Y.; Lipowska, M.; Christoforou, A. M.; Marzilli, L. G.; Taylor, A. T. *Nucl. Med. Biol.* **2007**, *34*, 709–716.
(3) Alberto, R.; Ortner, K.; Wheatley, N.; Schibli, R.; Schubiger, A. P. *J. Am. Chem. Soc.* **2001**, *123*, 3135–3136.
(4) Alberto, R.; Schibli, R.; Egli, A.; Schubiger, A. P.; Abram, U.; Kaden, T. A. *J. Am. Chem. Soc.* **1998**, *120*, 7987–7988.
(5) He, H.; Lipowska, M.; Xu, X.; Taylor, A. T.; Carlone, M.; Marzilli, L. G. *Inorg. Chem.* **2005**, *44*, 5437–5446.
(6) Schibli, R.; Schubiger, A. P. *Eur. J. Nucl. Med. Mol. Imaging* **2002**, *29*, 1529–1542.
(7) Schibli, R.; Schwarzbach, R.; Alberto, R.; Ortner, K.; Schmalle, H.; Dumas, C.; Egli, A.; Schubiger, A. P. *Bioconjugate Chem.* **2002**, *13*, 750–756.
(8) Causey, P. W.; Besanger, T. R.; Schaffer, P.; Valliant, J. F. *Inorg. Chem.* **2008**, *47*, 8213–8221.
(9) Schibli, R.; Bella, R. L.; Alberto, R.; Garcia-Garayoa, E.; Ortner, K.; Abram, U.; Schubiger, A. P. *Bioconjugate Chem.* **2000**, *11*, 345–351.

Published on Web 05/20/2010

Chart 1

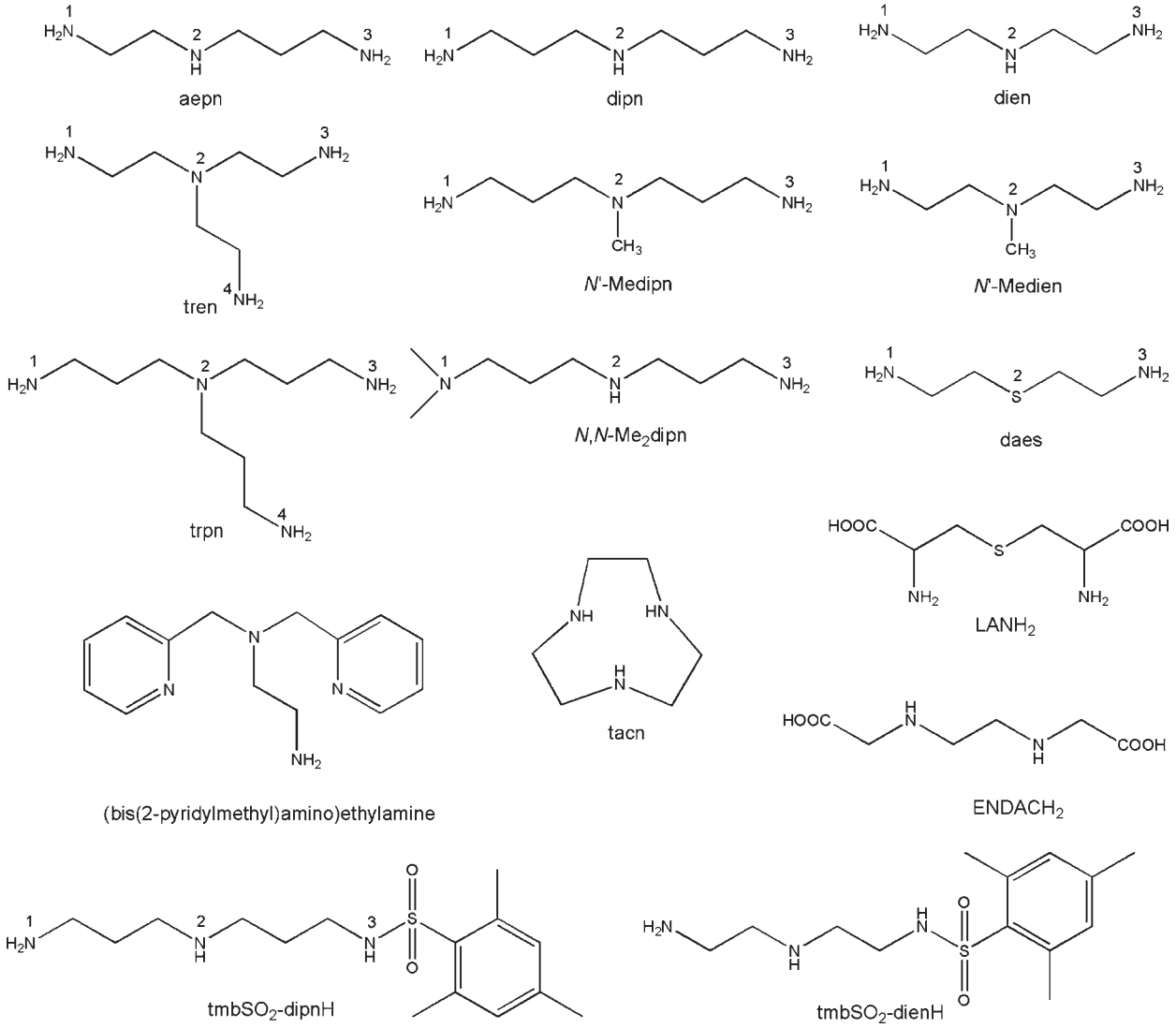

are widely used.[9−13] Ligands with carboxyl groups on dangling chains are normally evaluated in renal tracer development because the interaction of the renal receptor with the carboxyl group is important for clearance of small peptides.[14−16] Tridentate ligands being investigated in bioconjugates or in tracers often have the dangling group attached to a central N anchoring the two chelate rings.[10,17−19] Thymidine derivatives functionalized at position N3 of the nucleobase and attached to ^{99m}Tc or Re by a chain dangling from the central N of diethylenetriamine (dien) are recognized as substrates by human thymidine kinase 1, a promising target for noninvasive imaging and therapy of malignant cells.[19] A recent report describes *fac*-[^{188}Re(CO)$_3$((bis(2-pyridylmethyl)amino)ethylamine)]Br, a ^{188}Re complex exhibiting promising biomedical properties and having a pyridyl-containing tridentate ligand with a dangling ethylamine group attached to the central N (Chart 1).[18] Ligands named or used in this report are depicted in Chart 1. The H atom at the end of an abbreviation for a ligand name in Chart 1 or in the designation of a complex indicates the number of acidic H atoms retained by the coordinated ligand, or in some cases, such as trenH [tris-(2-aminoethyl)amine], the H atom indicates that the coordinated ligand has become protonated.

Highly functionalized *fac*-[Re(CO)$_3$L]^n complexes are difficult to crystallize, and also the solution structures relevant to the likely structure of the tracer may differ from that in solution. For example, dangling uncoordinated carboxyl groups (which are negatively charged and deprotonated at physiological pH) usually become neutral protonated groups

(10) Bartholomä, M.; Valliant, J.; Maresca, K. P.; Babich, J.; Zubieta, J. *Chem. Commun.* (*Cambridge, U.K.*) **2009**, *5*, 493–512.
(11) Maresca, K. P.; Kronauge, J. F.; Zubieta, J.; Babich, J. *Inorg. Chem. Commun.* **2007**, *10*, 1409–1412.
(12) Storr, T.; Fisher, C. L.; Mikata, Y.; Yano, S.; Adam, M. J.; Orvig, C. *Dalton Trans.* **2005**, 654–655.
(13) Tzanopolou, S.; Pirmettis, I. C.; Patsis, G.; Paravatou-Petsotas, M.; Livaniou, E.; Papadopoulos, M.; Pelecanou, M. *J. Med. Chem.* **2006**, *49*, 5408–5410.
(14) Trejtnar, F.; Laznicek, M. *Q. J. Nucl. Med.* **2002**, *46*, 181–194.
(15) Nosco, D. L.; Beaty-Nosco, J. A. *Coord. Chem. Rev.* **1999**, *184*, 91–12391.
(16) Shikano, N.; Kanai, Y.; Kawai, K.; Ishikawa, N.; Endou, H. *J. Nucl. Med.* **2004**, *45*, 80–85.
(17) Lipowska, M.; Marzilli, L. G.; Taylor, A. T. *J. Nucl. Med.* **2009**, *50*, 454–460.
(18) Xia, J.; Wang, Y.; Li, G.; Yu, J.; Yin, D. *J. Radioanal. Nucl. Chem.* **2009**, *279*, 245–252.
(19) Desbouis, D.; Struthers, H.; Spiwok, V.; Küster, T.; Schibli, R. *J. Med. Chem.* **2008**, *51*, 6689–6698.

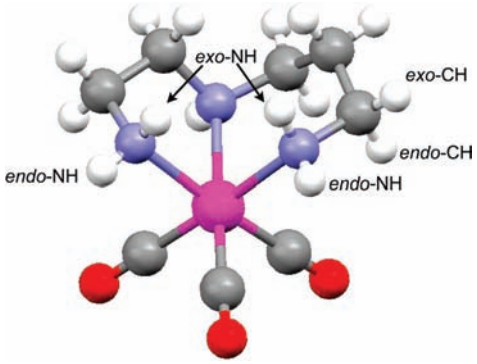

Figure 1. Designation of endo and exo protons in five-membered (left) and six-membered (right) rings, as illustrated based on the molecular structure of $[Re(CO)_3(aepn)]PF_6$. The *exo*-NH or *exo*-CH protons point away from the carbonyl ligands, and the *endo*-NH or *endo*-CH protons point toward the carbonyl ligands.

in procedures employed to crystallize the complex.[1,2,20−22] One goal of our study is to interpret how NMR spectra inform us about the solution structure of *fac*-$[Re(CO)_3L]^n$ complexes. We first became aware that an unusually wide shift range exists for NH signals at amine groups terminating chelate rings (i.e., amines not anchoring two chelate rings) in *fac*-$[Re(CO)_3L]^n$ complexes in a study of two *fac*-$[Re(CO)_3$-(ENDACH)] isomers (the $ENDACH_2$ ligand shown in Chart 1).[21] For both isomers in the solid state, the coordinated carboxyl group is deprotonated, whereas the dangling carboxyl group is protonated. Two types of terminal NH groups were defined and unambiguously identified through crystallography of the two isomers. In one isomer, the terminal amine has an *endo*-NH proton (defined as the proton projecting *toward* the carbonyl ligands; Figure 1) with a normal relatively downfield shift (5.84 ppm, DMSO-d_6) for a terminal secondary amine NH signal. In the other isomer, this amine has an *exo*-NH proton (defined as the proton projecting *away* from the carbonyl ligands; Figure 1).[21] The signal of this terminal secondary amine *exo*-NH proton was observed at a rather upfield position (5.36 ppm, DMSO-d_6).

In later studies,[1,5,23] we found a relatively wide range of NH shifts also for terminal primary amine groups in *fac*-[Re-$(CO)_3L]^+$ complexes.[1,23] When L = lanthionine isomers as the tridentate ligand ($LANH_2$; Chart 1), the *fac*-$[Re(CO)_3$-$(LAN)]^-$ isomers exhibited NH signals differing in shift, but the shift range was not readily understood.[1] For some primary amine groups, the two NH signals were well dispersed, whereas for others, the shifts of both NH signals were similar.[1] Because the two deprotonated dangling carboxyl groups of the *fac*-$[Re(CO)_3(LAN)]^-$ complex could be influencing the shift, we examined *fac*-$[Re(CO)_3L]^+$ complexes with such minimal prototypical ligands as dien or simple dien-related ligands (e.g., daes, Chart 1) to establish baseline chemical shift characteristics that define NMR parameters for *fac*-$[Re(CO)_3L]^n$ complexes.[24]

For the prototypical *fac*-$[Re(CO)_3L]^+$ complexes, with L lacking dangling groups and forming two five-membered rings, downfield and upfield NH signals were observed and assigned to *endo*-NH and *exo*-NH protons, respectively.[24] We hypothesized that the shift differences might be attributable, in part, to lower exposure to solvent of the *exo*-NH protons compared to the *endo*-NH protons. We reasoned that the chelate rings forming the face defined by L might provide a steric barrier that inhibits full access of the polyatomic solvent molecules to *exo*-NH protons. As a result, the solvent cannot approach *exo*-NH protons closely enough to allow the formation of strong solvent-to-NH hydrogen-bonding interactions (an interaction causing downfield shifts).[24] Therefore, we evaluated the interaction of the small monatomic Cl^- anion with these prototypical complexes.[24] We reasoned that the Cl^- anion would be attracted to the cationic complex, leading to an ion pair with the Cl^- anion hydrogen-bonded preferentially to the poorly solvated *exo*-NH groups. This interaction caused larger downfield shifts for the *exo*-NH signal than for the *endo*-NH signal, consistent with our hypothesis that solvent molecules are too large to access the *exo*-NH groups well. The extent of solvent accessibility to *exo*-NH groups might be altered by dangling groups on the ligands, by replacement of one of the groups with other donor types, by the chelate ring size, as well as by other possible factors.

In the present study, we investigate *fac*-$[Re(CO)_3L]^{n+}$ complexes bearing polyamine ligands having six-membered chelate rings to determine if some of the same unusual NH shifts are present in the ^1H NMR spectra of these compounds. Also, we test further our proposal that at least a significant factor influencing the shift is solvent exposure by assessing the interaction of anions of increasing size along the series Cl^-, Br^-, and I^-. We also evaluated the large paramagnetic Re^{IV} anion, $[ReBr_6]^{2-}$. This series of studies was designed to test the solvent exposure hypothesis that small species are expected to access the sterically hindered face of the octahedron defined by the tridentate ligand better than larger anions. Two-dimensional NMR NH signal assignment is more straightforward for *fac*-$[Re(CO)_3L]^{n+}$ complexes bearing polyamine ligands having two six-membered chelate rings than for *fac*-$[Re(CO)_3L]^{n+}$ complexes bearing polyamine ligands having five-membered chelate rings because ring pucker in the latter types of compounds is usually very fluxional and different for the two chelate rings.[24] From now on, we omit the fac designation when discussing specific compounds because all of the new compounds have this geometry.

Experimental Section

Starting Materials. Tris(2-aminoethyl)amine (tren), *N*-3-(aminopropyl)-1,3-propanediamine (dipn), *N*-2-(aminoethyl)-1,3-propanediamine (aepn), 3,3′-diamino-*N*-methyldipropylamine (*N*′-Medipn), *N*,*N*-dimethyldipropylenetriamine (*N*,*N*-Me_2dipn), tris(3-aminopropyl)amine (trpn), 1,4,7-triazacyclononane (tacn), and $Re_2(CO)_{10}$ from Aldrich were used as received. $[Re(CO)_3$-$(H_2O)_3]OTf$ (OTf = trifluoromethanesulfonate) and $[Bu_4N]_2$-$[ReBr_6]$ were prepared by known methods.[5,25]

NMR Measurements. ^1H (400 MHz) and ^2H (unlocked) NMR spectra were recorded on Bruker spectrometers. Peak

(20) Lipowska, M.; Hansen, L.; Xu, X.; Marzilli, P. A.; Taylor, A. T.; Marzilli, L. G. *Inorg. Chem.* **2002**, *41*, 3032–3041.
(21) Lipowska, M.; Cini, R.; Tamasi, G.; Xu, X.; Taylor, A. T.; Marzilli, L. G. *Inorg. Chem.* **2004**, *43*, 7774–7783.
(22) Hansen, L.; Lipowska, M.; Meléndez, E.; Xu, X.; Hirota, S.; Taylor, A. T.; Marzilli, L. G. *Inorg. Chem.* **1999**, *38*, 5351–5358.
(23) Christoforou, A. M.; Fronczek, F. R.; Marzilli, P. A.; Marzilli, L. G. *Inorg. Chem.* **2007**, *46*, 6942–6949.
(24) Christoforou, A. M.; Marzilli, P. A.; Fronczek, F. R.; Marzilli, L. G. *Inorg. Chem.* **2007**, *46*, 11173–11182.
(25) Maverick, A. W.; Lord, M. D.; Yao, Q.; Henderson, L. J. *Inorg. Chem.* **1991**, *30*, 554–558.

positions are relative to tetramethylsilane (TMS) by using TMS or in some cases a solvent residual peak referenced in turn to TMS. NMR data were processed with *TopSpin* and *Mestre-C* software.

X-ray Data Collection and Structure Determination. Intensity data were collected at 90.0(5) K on a Nonius Kappa CCD diffractometer fitted with an Oxford Cryostream cooler and graphite-monochromated Mo Kα (λ = 0.710 73 Å) radiation. Data reduction included absorption corrections by the multi-scan method, with HKL SCALEPACK.[26]

All X-ray structures were determined by direct methods and difference Fourier techniques and refined by full-matrix least squares, using *SHELXL97*.[27] All non-H atoms were refined anisotropically, except for those in the six-membered chelate rings of **5**, which were disordered into two conformations. Except for those on the water molecule in **1**, all H atoms were visible in difference maps. H atoms on C and N were placed in idealized positions, except for the NH H atoms in **2**, **4**, and **6**. A torsional parameter was refined for each methyl group. Compound **1** has three independent Re complexes in the asymmetric unit, two of which have disordered $(CH_2)_3$ groups. Compound **3** has two formula units in the asymmetric unit. Compound **7** crystallizes in a chiral conformation as an enantiopure crystal, as evidenced by Flack parameter $x = 0.014(6)$.

Synthesis of *fac*-[Re(CO)$_3$L]PF$_6$ and *fac*-[Re(CO)$_3$L]BF$_4$ Complexes. An aqueous solution of $[Re(CO)_3(H_2O)_3]$OTf (5 mL, 0.1 mmol) was treated with the ligands L (0.1 mmol). The pH was adjusted to ~6 (3 mL of methanol was added to dissolve any precipitate that formed), and the clear reaction mixture was heated at reflux for 16 h. The reaction mixture was allowed to cool to room temperature, treated with solid $NaPF_6$ or $NaBF_4$ (~15 mg), and then left undisturbed. X-ray-quality crystals formed within 2−3 days. Specific procedures are detailed below.

[Re(CO)$_3$(dipn)]BF$_4$ (1). The treatment of $[Re(CO)_3(H_2O)_3]$OTf with dipn (15 μL), as described above, afforded $[Re(CO)_3$(dipn)]BF_4 as colorless crystals (17 mg, 35% yield) after the addition of $NaBF_4$. The product was characterized by single-crystal X-ray diffraction. ^{1}H NMR spectrum (ppm) in DMSO-d_6: 6.00 (b, 1H, NH), 5.23 (d, 2H, NH), 3.79 (b, 2H, NH), 3.20 (m, 2H, CH_2), 2.90 (m, 2H, CH_2), 2.68 (m, 2H, CH_2), 2.62 (m, 2H, CH_2), 1.88 (m, 2H, CH_2), 1.68 (m, 2H, CH_2). **[Re(CO)$_3$(dipn)]PF$_6$.** The treatment of $[Re(CO)_3(H_2O)_3]$OTf with dipn, as described above, afforded $[Re(CO)_3$(dipn)]PF_6 as colorless crystals (36 mg, 66% yield) after the addition of $NaPF_6$. The product could not be characterized by single-crystal X-ray diffraction because of twinning. ^{1}H NMR spectrum (ppm) in DMSO-d_6: identical with that of $[Re(CO)_3$(dipn)]BF_4.

[Re(CO)$_3$(*N*′-Medipn)]PF$_6$ (2). The treatment of $[Re(CO)_3(H_2O)_3]$OTf with *N*′-Medipn (17 μL), as described above, afforded $[Re(CO)_3$(*N*′-Medipn)]PF_6 as colorless crystals (18 mg, 32% yield) after the addition of $NaPF_6$. The product was characterized by single-crystal X-ray diffraction. ^{1}H NMR spectrum (ppm) in DMSO-d_6: 5.30 (d, 2H, NH), 3.80 (t, 2H, NH), 3.20 (m, 2H, CH_2), 3.02 (m, 2H, CH_2), 2.98 (s, 3H, CH_3), 2.65 (m, 4H, CH_2), 1.90 (m, 2H, CH_2), 1.88 (m, 2H, CH_2).

[Re(CO)$_3$(*N*,*N*-Me$_2$dipn)]BF$_4$ (3). The treatment of $[Re(CO)_3(H_2O)_3]$OTf with *N*,*N*-Me$_2$dipn (18 μL), as described above, afforded $[Re(CO)_3$(*N*,*N*-Me$_2$dipn)]BF_4 as colorless crystals (29 mg, 56% yield) after the addition of $NaBF_4$. The product was characterized by single-crystal X-ray diffraction. ^{1}H NMR spectrum (ppm) in DMSO-d_6: 6.34 (s, 1H, NH), 5.53 (d, 1H, NH), 3.78 (t, 1H, NH), 3.24 (m, 1H, CH_2), 3.01 (s, 3H, CH_3), 2.90 (m, 3H, CH_2), 2.80 (m, 1H, CH_2), 2.71 (m, 3H, CH_2), 2.62 (s, 3H, CH_3), 1.94 (m, 1H, CH_2), 1.86 (m, 1H, CH_2), 1.62 (m, 2H, CH_2).

[Re(CO)$_3$(trenH)](PF$_6$)$_2$ (4). The treatment of $[Re(CO)_3(H_2O)_3]$OTf with tren (16 μL), as described above, afforded $[Re(CO)_3$(trenH)]$(PF_6)_2$ as colorless crystals (34 mg, 47% yield) after the addition of $NaPF_6$. The product was characterized by single-crystal X-ray diffraction. ^{1}H NMR spectrum (ppm) in DMSO-d_6: 7.70 (b, 3H, NH), 5.62 (b, 2H, NH), 4.22 (b, 2H, NH), 3.57 (m, 2H, CH_2), 3.18 (m, 2H, CH_2), 3.09 (m, 2H, CH_2), 2.91 (m, 6H, CH_2).

[Re(CO)$_3$(trpnH)](PF$_6$)$_2$ (5). The treatment of $[Re(CO)_3(H_2O)_3]$OTf with trpn (20 μL), as described above, afforded $[Re(CO)_3$(trpnH)]$(PF_6)_2$ as colorless crystals (34 mg, 45% yield) after the addition of $NaPF_6$. The product was characterized by single-crystal X-ray diffraction. ^{1}H NMR spectrum (ppm) in DMSO-d_6: 7.69 (b, 3H, NH), 5.39 (b, 2H, NH), 3.72 (b, 2H, NH), 3.10 (m, 4H, CH_2), 2.85 (m, 4H, CH_2), 2.75 (m, 4H, CH_2), 1.96 (m, 6H, CH_2).

[Re(CO)$_3$(aepn)]PF$_6$ (6). The treatment of $[Re(CO)_3(H_2O)_3]$OTf with aepn (13 μL), as described above, afforded $[Re(CO)_3$(aepn)]PF_6 as colorless crystals (30 mg, 56% yield) after the addition of $NaPF_6$. The product was characterized by single-crystal X-ray diffraction. ^{1}H NMR spectrum (ppm) in DMSO-d_6: 6.47 (b, 1H, NH), 5.50 (d, 1H, NH), 5.24 (d, 1H, NH), 4.08 (b, 1H, NH), 3.50 (t, 1H, NH), 3.25 (m, 1H, CH_2), 3.04 (m, 1H, CH_2), 2.97 (m, 1H, CH_2), 2.63 (m, 3H, CH_2), 2.57 (m, 1H, CH_2), 2.43 (m, 1H, CH_2), 1.94 (m, 1H, CH_2), 1.74 (m, 1H, CH_2).

[Re(CO)$_3$(tacn)]PF$_6$ (7). The treatment of $[Re(CO)_3(H_2O)_3]$OTf with tacn (13 mg), as described above, afforded $[Re(CO)_3$(tacn)]PF_6 as colorless crystals (30 mg, 55% yield) after the addition of $NaPF_6$. The product was characterized by single-crystal X-ray diffraction. ^{1}H NMR spectrum (ppm) in DMSO-d_6: 7.06 (b, 3H, NH), 2.96 (m, 6H, CH_2), 2.88 (m, 6H, CH_2).

Cl$^-$ Titration of [Re(CO)$_3$L]PF$_6$ Complexes. A 5 mM solution of the desired *fac*-$[Re(CO)_3L]PF_6$ complex in DMSO-d_6 or acetonitrile-d_3 (600 μL) was treated with increasing amounts of Et_4NCl (1−125 mM), and the solution was monitored by ^{1}H NMR spectroscopy after each Cl^- aliquot was added. All Et_4NCl stock solutions were prepared by using a 5 mM solution of the complex to keep the complex concentration constant throughout the titration. Similar experiments were performed with $[Re(CO)_3$(dipn)]PF_6 in acetonitrile-d_3 by using Et_4NBr (1−125 mM) and Et_4NI (1−50 mM, owing to low solubility).

Preparation of [Re(CO)$_3$(dipn-*d*$_5$)]PF$_6$. The NH NMR signals of a 5 mM solution of $[Re(CO)_3$(dipn)]PF_6 in acetonitrile-d_3 (600 μL) disappeared within ~40 min after the addition of D_2O (5 μL) and K_2CO_3 (2 mg). Therefore, the NH groups of $[Re(CO)_3$(dipn)]PF_6 (8 mg) in CH_3CN (3 mL) were exchanged by using D_2O (70 μL) and K_2CO_3 (8 mg). The reaction mixture was taken to dryness, the residue dissolved in CH_3CN, and the solution filtered to remove K_2CO_3. The filtrate was taken to dryness, and the residue was redissolved in CH_3CN (3 mL) to give a 5 mM $[Re(CO)_3$(dipn-d_5)]PF_6 stock solution for use in ^{2}H NMR monitored titrations. Later, $[Re(CO)_3$(dipn-d_5)]PF_6 was prepared more conveniently by using the volatile Et_3N instead of K_2CO_3.

Addition of [Bu$_4$N]$_2$[ReBr$_6$] to [Re(CO)$_3$(dipn-*d*$_5$)]PF$_6$. A 5 mM solution of $[Re(CO)_3$(dipn-d_5)]PF_6 in CH_3CN (600 μL) was treated with increasing amounts of $[Bu_4N]_2[ReBr_6]$ (1−12 mM), and the solution was monitored by ^{2}H NMR spectroscopy after each $[ReBr_6]^{2-}$ aliquot was added. An analogous ^{1}H NMR experiment was performed with $[Re(CO)_3$(dipn)]PF_6 in acetonitrile-d_3. The $[Re(CO)_3$(dipn-d_5)]PF_6 concentration was kept constant throughout the titrations, as described above.

Results and Discussion

Synthesis. A $[Re(CO)_3(H_2O)_3]$OTf aqueous solution[5] (pH ~ 6) was used to prepare all of the complexes crystallized and structurally characterized in this study (Scheme 1). All complexes are new except for the tacn

(26) Otwinowski, Z.; Minor, W. *Macromolecular Crystallography, part A, Methods in Enzymology*; New York Academic Press: New York, 1997; Vol. *276*, pp 307−326.

(27) Sheldrick, G. M. *Acta Crystallogr., Sect. A* **2008**, *A64*, 112–122.

Scheme 1

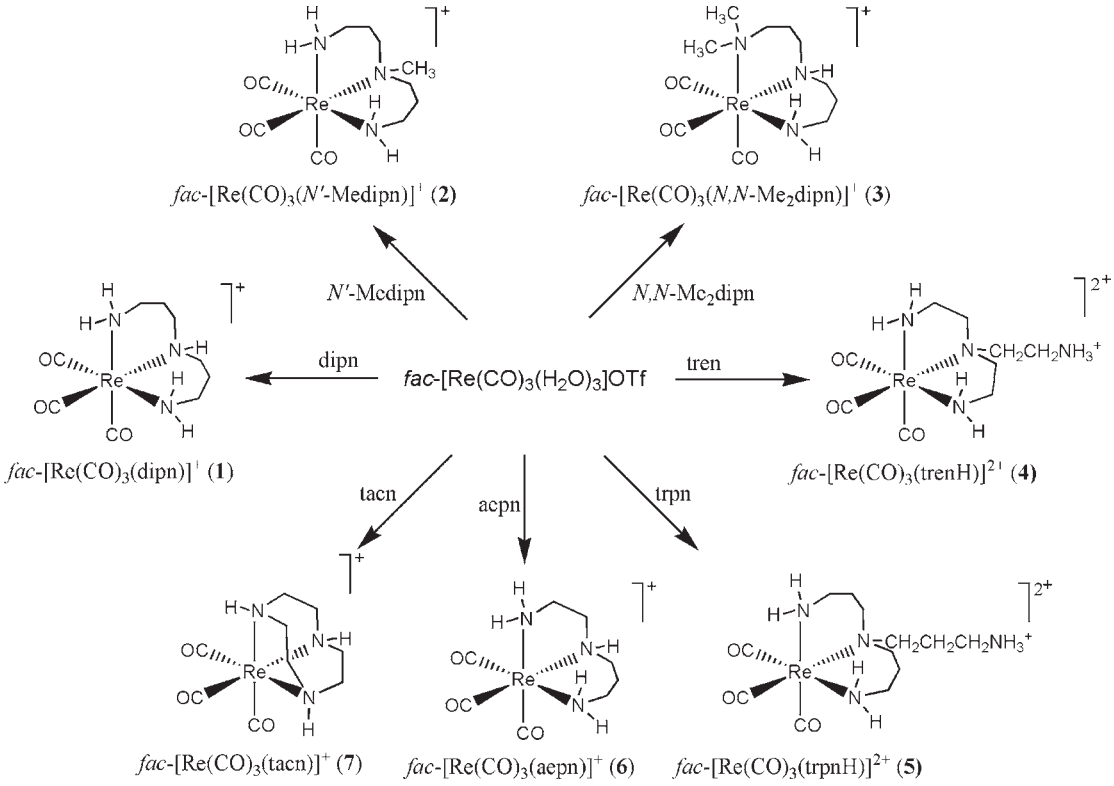

complex, which was not previously characterized as a PF_6^- salt.[28,29] This salt was needed for our NMR studies.

X-ray Crystallography. All complexes possess a distorted octahedral structure, with the three carbonyl ligands occupying one face. The three remaining coordination sites are occupied by amine N atoms (Figures 2−4). Crystal data and details of the structural refinement for these complexes are summarized in Table 1. Ligands and their abbreviations are depicted in Chart 1. The complexes have chelate rings of different sizes: two six-membered chelate rings ($[Re(CO)_3(dipn)]BF_4$ (**1**), $[Re(CO)_3(N'\text{-Medipn})]PF_6$ (**2**), $[Re(CO)_3(N,N\text{-Me}_2dipn)]BF_4$ (**3**), and $[Re(CO)_3(trpnH)](PF_6)_2$ (**5**)); six- and five-membered chelate rings ($[Re(CO)_3(aepn)]PF_6$ (**6**)); two five-membered rings ($[Re(CO)_3(trenH)](PF_6)_2$ (**4**)); or three five-membered rings ($[Re(CO)_3(tacn)]PF_6$ (**7**)). For all complexes except $[Re(CO)_3(tacn)]PF_6$ (**7**), N1 and N3 refer to bound terminal N atoms of the ligand and N2 denotes the central N atom; for $[Re(CO)_3(trenH)](PF_6)_2$ (**4**) and $[Re(CO)_3(trpnH)](PF_6)_2$ (**5**), the N atom of the dangling NH_3^+ group is designated as N4 (Chart 1).

Selected Re−N bond lengths and the N−Re−N bond angles are summarized in Table 2. The Re−N bond lengths and N−Re−N bond angles are consistent with those found in similar *fac*-$[Re(CO)_3L]^+$ complexes.[23,24] It is useful to compare the N−Re−N angles for two terminal amine groups of $[Re(CO)_3(dien)]PF_6$ [87.14(12)°], which has two five-membered chelate rings,[24] with those of $[Re(CO)_3(aepn)]PF_6$ [86.74(15)°], which has five- and six-membered chelate rings (Figure 2), and $[Re(CO)_3(dipn)]BF_4$ [84.67(10)°], which has two six-membered rings (Figure 2). The N−Re−N angle relating two terminal N atoms decreases significantly as the ring size increases (Table 2). The nonbonded distances between N1 and N3 are mostly similar for complexes **1**−**6**, ranging from 3.01 to 3.14 Å (Table 3) regardless of the size of the chelate ring.

The presence of a methyl group on N2 of **2** is reflected in a longer Re−N2 bond distance for **2** [2.299(2) Å] than for **1** [2.244(3) Å; Table 2]. A similar difference in the Re−N2 bond distance is found for the corresponding complexes with two five-membered rings (L = dien and *N*′-Medien; Chart 1).[24] Thus, in $[Re(CO)_3L]^{n+}$ complexes containing either six- or five-membered chelate rings, having a methyl substituent on N2 increases the Re−N2 bond distance by a similar small extent. This same conclusion appears to apply when data for **4** and **5** are considered. The central N in **4** and **5** bears a $CH_2CH_2NH_3^+$ group; the greater bulkiness of this dangling group does not appear to cause any greater lengthening of the Re−N2 bond than does the methyl group.

Chelate Ring Conformation. In the next subsection on NMR signal assignments, we discuss the use of COSY NMR spectra and chelate ring torsion angles, which depend on chelate ring conformation. Thus, it is useful to consider chelate ring conformations in the new structures and to compare these to conformations found in previous studies.[23,24] From Scheme 1, it can be seen that all of the new complexes except **3** and **6** will have a time-averaged plane of symmetry. However, none have such a plane in the solid state (Figures 2 and 3).

The N2,N3 six-membered rings in compounds **1**−**3** and **6** (Figure 2) all have very similar chair conformations

(28) Wieghardt, K.; Pomp, C.; Nuber, B.; Weiss, J. *Inorg. Chem.* **1986**, *25*, 1659–1661.
(29) Suzuki, K.; Shimmura, N.; Thipyapong, K.; Uehara, T.; Akizawa, H.; Arano, Y. *Inorg. Chem.* **2008**, *47*, 2593–2600.

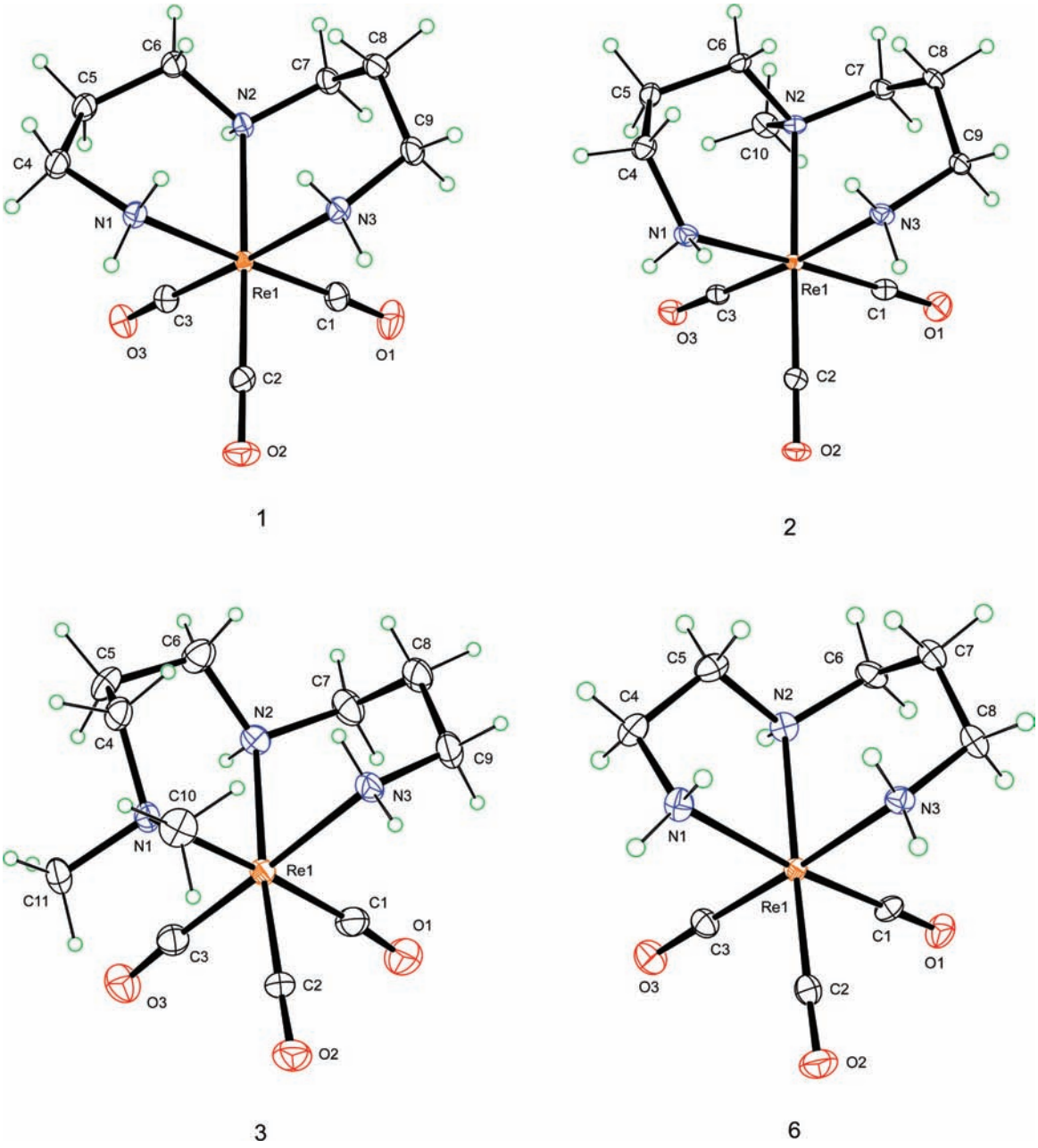

Figure 2. ORTEP plots of the cations of **1**−**3** and **6**. Thermal ellipsoids are drawn with 50% probability. Only one of the independent molecules is shown for **1** ($z' = 3$) and **3** ($z' = 2$).

(Chart 2). However, the conformation of the N1,N2 ring differs; this ring has the twist-boat conformation in **1** (Chart 2), the sofa conformation in **2** and **3** (Chart 2), and five members in **6** (see below).[30,31]

When the two chelate rings are not equivalent (as in **3** and **6**), L has a "head" and a "tail" (htL), and thus the complex is chiral. Also, one of the htL rings may dictate the conformation of the other ring. For **3**, in which both rings are six-membered and flexible, such conformational control of one ring by the other ring is not evident.

In contrast, when one htL ring is five-membered, the conformation of the ring may be influenced by the other ring. The conformation of five-membered rings is described by ring pucker (λ or δ; Figure 5). One ring pucker (λ or δ) may be favored. In cases such as [$Re(CO)_3$(tmbSO$_2$-dien)], in which both rings of the htL are five-membered, this chirality will determine the favored ring pucker of each ring (λ or δ).[23] The common pucker designation (λ or δ) is not useful for interpreting NMR data. Instead, we designate the five-membered ring conformations as *endo*-C and *exo*-C, where the ring C bound to the terminal N projects toward and away, respectively, from the carbonyl ligands (Figure 5). This designation can also be used for six-membered rings (Figure 5). Please note that the ring C has both an *endo*-CH and an *exo*-CH, regardless of whether or not the C atom is an *endo*-C or an *exo*-C. For example, in Figure 1, the six-membered ring shown has an *endo*-C with its two H atoms labeled as *endo*-CH and *exo*-CH.

(30) DaCruz, M. F.; Zimmer, M. *Inorg. Chem.* **1998**, *37*, 366–368.
(31) Bérces, A.; Whitfield, D. M.; Nukada, T. *Tetrahedron* **2001**, *57*, 477–491.

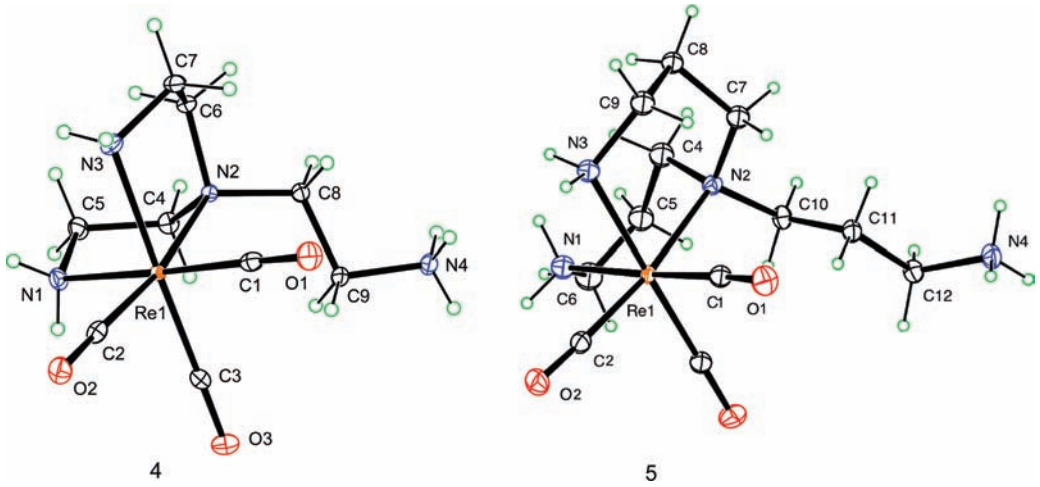

Figure 3. ORTEP plots of the cations of **4** and **5**. Thermal ellipsoids are drawn with 50% probability.

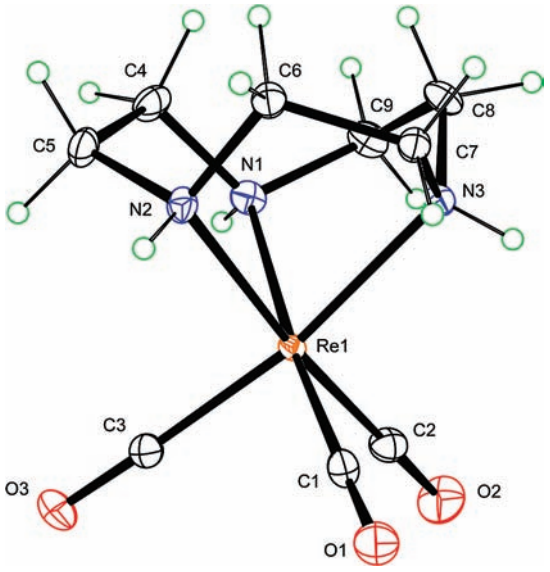

Figure 4. ORTEP plot of the cation of **7**. Thermal ellipsoids are drawn with 50% probability.

NMR Spectroscopy. Complexes **1**−**7** were characterized by NMR spectroscopy in DMSO-d_6 (Figures 6 and S1 in the Supporting Information), acetonitrile-d_3, and acetone-d_6 at 25 °C (Table 4). COSY experiments performed for most of the complexes at 25 °C in DMSO-d_6, together with torsion angles obtained from the respective molecular structures, were useful in assigning NMR signals.

In our previous work, the assignment by COSY or other means of an NH signal to an *exo*-NH or *endo*-NH proton was possible either because the complex contained only one of these types of protons in a secondary amine or because there was only one NH_2 group in a unique five-membered chelate ring (the ligand was an htL).[23] For example, the ring with the terminal amine in $[Re(CO)_3(tmbSO_2\text{-dien})]$ has an *exo*-C conformation in the solid, and the *endo*-NH signal exhibited a strong COSY cross-peak to the *exo*-CH signal. In **6**, the five-membered chelate ring has an *endo*-C conformation, and the *exo*-NH signal exhibited a strong COSY cross-peak to the *endo*-CH signal of the adjacent (*endo*) methylene group.

For a symmetric (non-htL) complex with two identical ethylene chains such as $[Re(CO)_3(dien)]^+$, the five-membered chelate rings undergo a rapid change in pucker, with both rings λ (λ,λ) or both δ (δ,δ).[24] Over time, any given CH_2 group in these rings is alternately endo or exo with respect to the carbonyl ligands. This rapid conformational interchange process averages the torsion angles such that *endo*-NH and *exo*-NH to CH couplings average. This averaging is found for each of the NH signals to both CH signals (unpublished data). COSY data cannot be used to assign the signals. However, the position in conformational space of the NH groups moves just slightly as the slight rotation about the Re−N bond occurs during the dynamic process. Thus, the *exo*-NH signal remains upfield to the *endo*-NH signal.[24]

The conformations of six-membered rings are more diverse than those of five-membered rings (Chart 2), as discussed above. However, the chair conformation is most commonly found for the six-membered rings in the new structures, and we assume that the solution structures will be dominated by this conformation, even in those symmetrical compounds in which the rings undergo conformational interchange. As will be seen, this assumption is justified by its utility in interpreting the NMR data. In the chair conformation, the *exo*-NH proton is related to the *endo*-CH proton by the largest H−N−C−H torsion angle (Table S1 and Figure S2 in the Supporting Information); thus, for the six-membered ring(s) in **1**−**3** and **6** (which exhibit similar COSY NH−CH cross-peaks), the NH−CH cross-peak having the highest intensity will be the *exo*-NH−*endo*-CH cross-peak (see below and the Supporting Information).

We begin our discussion with **3** (Figure 2), a chiral complex with an unsymmetrically coordinated htL in which dynamic motion cannot interchange the rings. The ring with the terminal NH_2 group has the chair conformation. The expected three NH signals (central NH and terminal NH_2) were observed for **3** in DMSO-d_6 (Table 4 and Figure S3 in the Supporting Information). COSY studies discussed in the Supporting Information establish that, although the chelate ring has six members, the *exo*-NH shift is upfield, as was found for five-membered chelate rings. However, the *exo*-NH−*endo*-CH COSY cross-peak is larger than the *endo*-NH−*exo*-CH

Table 1. Crystal Data and Structure Refinement for **1**−**7**

	1	**2**	**3**	**4**	**5**	**6**	**7**
empirical formula	$C_9H_{17}N_3O_3Re\cdot BF_4\cdot 0.33H_2O$	$C_{10}H_{19}N_3O_3Re\cdot PF_6$	$C_{11}H_{21}N_3O_3Re\cdot BF_4$	$C_9H_{19}N_4O_3Re\cdot(PF_6)_2\cdot H_2O$	$C_{12}H_{25}N_4O_3Re\cdot(PF_6)_2$	$C_8H_{15}N_3O_3Re\cdot PF_6$	$C_9H_{15}N_3O_3Re\cdot PF_6$
fw	494.27	560.45	516.32	725.44	749.50	532.40	544.41
space group	$P2_1/c$	$P\bar{1}$	*Pbca*	$P2_1/n$	*Pnma*	*Pbca*	$P2_1$
a (Å)	21.2819(15)	8.3290(10)	14.546(2)	7.8157(5)	29.620(2)	13.2550(15)	8.1859(10)
b (Å)	13.1010(5)	8.4008(10)	13.335(2)	13.7565(10)	9.5359(5)	12.756(2)	12.5249(15)
c (Å)	16.0615(10)	11.8149(15)	34.811(6)	18.9670(15)	7.9455(5)	17.512(3)	8.3319(10)
α (deg)	90	87.892(7)	90	90	90	90	90
β (deg)	94.218(2)	84.975(6)	90	91.516(4)	90	90	117.085(4)
γ (deg)	90	89.380(7)	90	90	90	90	90
V (Å^3)	4466.0(5)	822.93(17)	6752.3(18)	2038.6(3)	2244.2(2)	2960.9(8)	760.57(16)
T (K)	90	90	90	90	90	90	90
Z	12	2	16	4	4	8	2
ρ_{calcd} (g/m^3)	2.205	2.262	2.032	2.364	2.218	2.389	2.377
abs coeff (mm^{-1})	8.22	7.56	7.25	6.25	5.68	8.40	8.18
$2\theta_{max}$ (deg)	71.4	66.4	57.6	72.6	71.2	65.8	82.0
R1 indices[a]	0.035	0.026	0.034	0.023	0.023	0.036	0.025
wR2 [$I > 2\sigma(I)$][b]	0.077	0.055	0.094	0.057	0.057	0.080	0.056
data/param	20 482/652	6238/231	8645/419	9583/317	5413/185	5417/215	9584/209

[a] $R = (\sum||F_o| - |F_c||)/\sum|F_o|$. [b] $wR2 = [\sum[w(F_o^2 - F_c^2)^2]/\sum[w(F_o^2)^2]]^{1/2}$, in which $w = 1/[\sigma^2(F_o^2) + (dP)^2 + (eP)]$ and $P = (F_o^2 + 2F_c^2)/3$, $d = 0.0356$, 0.0245, 0.0412, 0.0241, 0.0294, 0.0225, and 0.0131 and $e = 7.9046$, 0.3934, 0.4422, 3.894, 2.1227, 2.1782, and 1.8054 for complexes **1**−**7**, respectively.

Table 2. Selected Bond Distances (Å) and Angles (deg) for **1**−**7**

	1	**2**	**3**	**4**	**5**	**6**	**7**
				Bond Distances			
Re−N1	2.235(3)	2.249(2)	2.306(4)	2.2218(17)	2.218(4)	2.210(4)	2.194(4)
Re−N2	2.244(3)	2.299(2)	2.245(4)	2.2687(16)	2.281(2)	2.229(4)	2.208(2)
Re−N3	2.236(3)	2.226(2)	2.215(4)	2.2173(17)	2.275(4)	2.234(4)	2.209(2)
				Bond Angles			
N1−Re−N2	84.72(10)	91.47(8)	91.82(14)	78.55(6)	83.62(13)	77.42(14)	77.10(11)
N2−Re−N3	85.57(10)	84.63(8)	81.80(15)	77.35(6)	86.11(12)	83.90(14)	77.14(8)
N1−Re−N3	84.67(10)	84.32(9)	87.88(14)	88.04(7)	88.80(18)	86.74(15)	77.34(11)

Table 3. Selected Nonbonded Distances (Å) for **1**−**7**

	1	**2**	**3**	**4**	**5**	**6**	**7**
			Nonbonded Distances				
N1,N2	3.018	3.257	3.269	2.843	3.000	2.776	2.744
N2,N3	3.043	3.047	2.920	2.804	3.110	2.983	2.755
N1,N3	3.012	3.005	3.137	3.085	3.143	3.052	2.751
exo-NH, *exo*-NH	2.112	2.475		2.571	2.336	2.314	

Chart 2

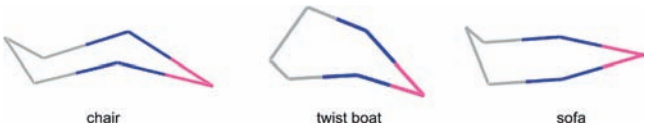

COSY cross-peak, unlike the case of the five-membered chelate ring of $[Re(CO)_3(tmbSO_2\text{-dien})]$ in a previous study in which the largest H−N−C−H torsion angle was ∼157° for a ring in the *exo*-C conformation (Figure 5). For this compound, the *endo*-NH−*exo*-CH cross-peak was the strongest HN−CH cross-peak.[23]

As was found for **3**, COSY data for **1** in DMSO-d_6 (Supporting Information) allowed us to establish that the *exo*-NH signal is upfield. Furthermore, unlike the case for symmetrical complexes with two five-membered rings, the NH signals of the complexes with two six-membered rings can be assigned unambiguously by COSY to either *exo*-NH or *endo*-NH. A COSY experiment on **6** in DMSO-d_6 showed NH−CH correlations (Supporting Information), which leave no doubt about the assignment of the NH signals (Figure 6) of the six-membered ring. NMR results indicate that six-membered rings in **1**−**3** and **6** have an *endo*-C conformation (Figure 5).

The COSY spectrum of **6** establishes that the pucker of the five-membered ring is *endo*-C in solution, the same conformation as that in the solid. Thus, the six-membered ring induces a preferred *endo*-C conformation in the five-membered ring in both the solution and solid states. Note that the ring bearing the $tmbSO_2$ group in the case of $[Re(CO)_3(tmbSO_2\text{-dien})]$ also induces a preferred ring conformation in both states, but this conformation is *exo*-C.[23]

For **4**, both five-membered chelate rings will time average between *endo*-C and *exo*-C conformations in solution. Thus, as expected for a symmetrical complex with two five-membered rings, the NH−CH COSY cross-peaks in DMSO-d_6 have similar intensities and do not allow assignment of the signals to a specific proton (Figure S4 in the Supporting Information). However, we can use the clear pattern that the upfield NH signal arises from the *exo*-NH proton to assign the NH signals of **4** (Table 4).

Factors Influencing Shifts of NH Signals for Six- versus Five-Membered Rings. Assignments and shifts of the NH signals of the new complexes in several solvents are summarized

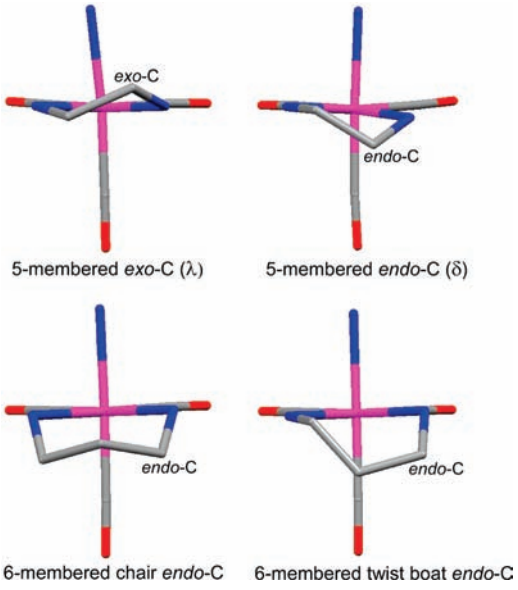

Figure 5. Designations of the *exo*-C and *endo*-C conformations for five- and six-membered rings of *fac*-$[Re(CO)_3L]^n$ complexes. Re is directed away from the viewer, and the N atoms are blue. The terminal N of the ring of interest is on the right, the central N is on the left, and the terminal N (but not the chain methylene groups) of the other ring is in the axial position. Note that, for five-membered rings, the chirality of the ring pucker is also designated.

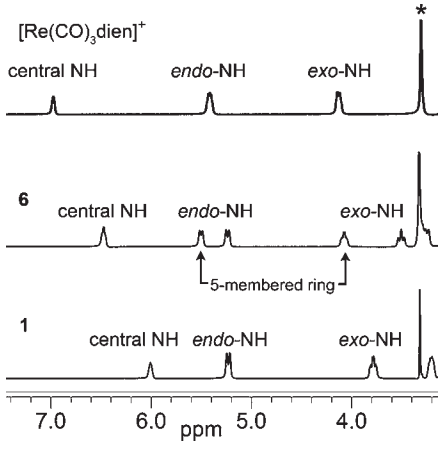

Figure 6. ^1H NMR spectra of **1**, **6**, and $[Re(CO)_3(dien)]PF_6$ (top) in DMSO-d_6 at 25 °C (the asterisk indicates the water peak). Full spectra for **1** and **6** are presented in Figure S1 in the Supporting Information.

in Table 4. Spectra are shown in Figure 6 and in the Supporting Information. An important goal of the current study is to understand factors influencing the NH shifts for six-membered rings. Our interest focuses on the dependence of shifts on through-space and solvent effects, and thus we must factor out the through-bond inductive effect on the shift of the extra methylene group in the six- versus five-membered rings of *fac*-$[Re(CO)_3L]^n$ complexes. The through-bond inductive effect is best assessed by considering the shift of the signal of the central NH group.

As illustrated in Figure 6, the central NH signal of $[Re(CO)_3(dipn)]^+$ in DMSO-d_6 is more upfield (6.01 ppm; Table 4) than that of $[Re(CO)_3(dien)]^+$ (6.98 ppm).[24] The more upfield shift of the NH signal of a central N joining six-membered rings than for an N joining five-membered

Table 4. Selected ^1H NMR Chemical Shifts (ppm) of **1**−**7** at 25 °C[a]

	1	2	3	4	5	6	7
				DMSO-d_6			
exo-NH	3.78	3.80	3.78	4.22	3.72	4.07, 3.50[c]	
endo-NH	5.22	5.30	5.53	5.62	5.39	5.50, 5.24[c]	
central NH	6.01		6.34	7.70[b]	7.69[b]	6.47	7.06
				Acetonitrile-d_3			
exo-NH	2.83	2.85	2.83	3.36	2.76	3.15, 2.53[c]	
endo-NH	4.18	4.22	4.36	4.44	4.27	4.37, 4.17[c]	
central NH	4.76		4.99	6.34[b]	6.22[b]	5.10	5.57
				Acetone-d_6			
exo-NH	3.83	3.90	3.76	4.36	3.76	4.14, 3.64[c]	
endo-NH	5.11	5.17	5.38	5.50	5.22	5.38, 5.10[c]	
central NH	5.67		5.98	4.49[b]	4.05[b]	6.13	6.62

[a] COSY spectra were used to assign the NH signals of **1**−**6** in DMSO-d_6 and **4** in acetone-d_6. [b] For **4** and **5**, the chemical shift of the dangling NH_3^+ group is listed in the rows containing central NH values. [c] The second entry is for the six-membered ring.

rings[24] can also be observed in acetonitrile-d_3 and acetone-d_6 (Table 4). Furthermore, the shift of the central NH of $[Re(CO)_3(aepn)]^+$ is 6.47 ppm; thus, the shift for the compound with one five-membered ring and one six-membered ring is almost exactly between the shifts for the 5,5 and 6,6 compounds. This relationship is also found for the central NH signal of $[Re(CO)_3(N,N\text{-}Me_2\text{-}dipn)]^+$ (6.34 ppm) versus that of its corresponding dien analogue, $[Re(CO)_3(N,N\text{-}Me_2dien)]^+$ (7.02 ppm).[24] Thus, there is an inductive through-bond, upfield-shifting effect of ∼0.3−0.5 ppm for every five- to six-membered ring change. This finding is also true for acetone-d_6 and acetonitrile-d_3, even though the specific values quoted above are for DMSO-d_6.

If this inductive effect alone were influencing the shifts of the *exo*-NH and *endo*-NH signals, then these also would be shifted upfield by ∼0.3−0.5 ppm for every five- to six-membered ring change (Figure 6). For $[Re(CO)_3(dipn)]^+$, in DMSO-d_6, the upfield *exo*-NH signal (3.78 ppm) is more upfield than the *exo*-NH signal for $[Re(CO)_3(dien)]^+$ (4.14 ppm),[24] and the *endo*-NH signal (5.22 ppm) is also more upfield than that for $[Re(CO)_3(dien)]^+$ (5.43 ppm).[24] A comparison of the NH shifts in DMSO-d_6 for this pair of complexes (Figure 6) and several more pairs of complexes [trpnH vs trenH (Supporting Information); *N*′-Medipn versus *N*′-Medien;[24] and *N*,*N*-Me_2dipn vs *N*,*N*-Me_2dien[24]] indicates that the *exo*-NH signal is upfield by an average of ∼0.4 ppm and the *endo*-NH signal is upfield by an average of ∼0.2 ppm for complexes with two six-membered rings versus those with two five-membered rings. We attribute these differences to the inductive effect and suggest that the effect on the signals of the terminal amine protons is smaller than that on central secondary amine NH signals. At present, not enough information exists to interpret the causes of these small differences, but it is clear that the shifts of the NH_2 signals of one chelate ring depend slightly on the features of the other chelate ring (cf. Figure 6).

The NH protons of **7** may be considered to resemble closely the central NH protons of rhenium tricarbonyl complexes containing five-membered rings such as $[Re(CO)_3(dien)]^+$. These NH protons are directed toward

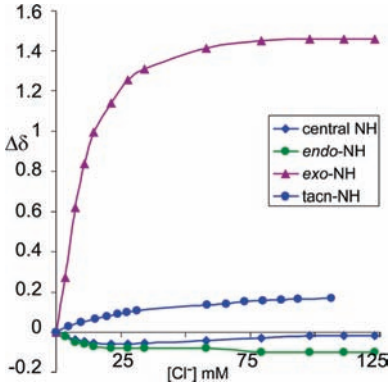

Figure 7. Effect of Cl^- on $\Delta\delta$ of the NH signals of **1** and **7** (designated as tacn-NH) in DMSO-d_6 at 25 °C.

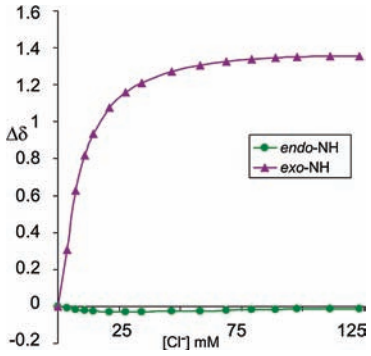

Figure 8. Effect of Cl^- on $\Delta\delta$ of the NH signals of **2** in DMSO-d_6 at 25 °C.

the solvent, away from the hydrophobic pocket. The ^1H NMR shifts of the NH signals of $[Re(CO)_3(tacn)]^+$ in DMSO-d_6 (7.06 ppm), acetonitrile-d_3 (5.57 ppm), and acetone-d_6 (6.62 ppm) are very similar to those of $[Re(CO)_3(dien)]^+$ (6.98, 5.57, and 6.57 ppm in DMSO-d_6, acetonitrile-d_3, and acetone-d_6, respectively).[24] Because $[Re(CO)_3(tacn)]^+$ lacks competing *exo*-NH and *endo*-NH protons, we use $[Re(CO)_3(tacn)]^+$ as a control to help interpret the effect of Cl^- upon the central NH signals of the new complexes in the studies to be described next.

Interaction of the *exo*-NH Groups with the Cl^- Anion. The effects of Cl^- addition on the NH shifts for 5 mM solutions of several complexes in DMSO-d_6 were assessed. Upon the addition of Et_4NCl, the observed shift changes, $\Delta\delta$, of the *exo*-NH signals of **1**, **2**, and **4**−**6** (Figures 7−9 and S5 and S6 in the Supporting Information) were downfield (positive values). (The smaller $\Delta\delta$'s for the *endo*-NH and central NH signals are discussed below.)

For **1**, the shift changes of the *exo*-NH signal ($\Delta\delta$ = ~1.4 ppm, plateau at $[Cl^-]$ of ~75 mM; Figure 7) were comparable to those for $[Re(CO)_3(dien)]^+$ ($\Delta\delta$ = ~1.2 ppm, plateau at $[Cl^-]$ of ~100 mM).[24] Following a reported treatment of the $\Delta\delta$ data,[24] we calculated the equilibrium constant for ion pairing ($[Re(CO)_3L]^{n+} + X^{m-} \leftrightarrow [Re(CO)_3L]^{n+},X^{m-}$) in DMSO-$d_6$ at 25 °C. A value of $168 \pm 26\ M^{-1}$ was calculated for the equilibrium constant for $[Re(CO)_3(dipn)]^+ + Cl^- \leftrightarrow [Re(CO)_3(dipn)]^+,Cl^-$. This value is comparable to that reported for $[Re(CO)_3(dien)]^+$ ($93 \pm 11\ M^{-1}$).[24] The nonbonded distance between the two *exo*-NH protons in **2**, a complex with two

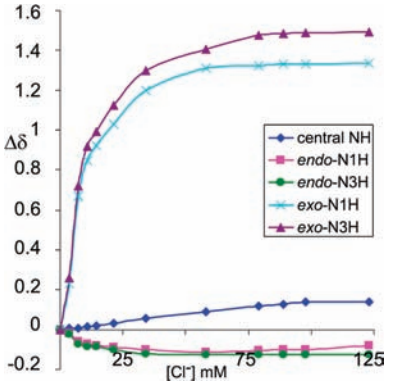

Figure 9. Effect of Cl^- on $\Delta\delta$ of the NH signals of **6** in DMSO-d_6 at 25 °C. A COSY spectrum was used to assign the NH signals.

representative six-membered conformations, is 2.475 Å, a value similar to the 2.509 Å distance in $[Re(CO)_3(dien)]PF_6$,[24] a representative compound with two five-membered chelate rings.

The standard method for calculating ion-pairing equilibrium constants in DMSO-d_6 gave values for the $[Re(CO)_3(aepn)]^+,Cl^-$ equilibrium of $210 \pm 12\ M^{-1}$ (*exo*-N1H $\Delta\delta$ plateau = 1.33 ppm) and $188 \pm 13\ M^{-1}$ (*exo*-N3H $\Delta\delta$ plateau = 1.49 ppm) for the NH protons. In the molecular structure of **6** (Figure 2), the distance between the two *exo*-NH protons is 2.314 Å. For **4**, this distance is 2.571 Å, and Cl^- ion pairing caused a large $\Delta\delta$ for the *exo*-NH proton (1.2 ppm). For **5**, the distance between the *exo*-NH protons is 2.336 Å and the *exo*-NH $\Delta\delta$ plateau = 1.5 ppm. However, the ion-pairing equilibrium constant could not be determined well, possibly because of the extra charge and the dangling charged group (see below).

The new results on *exo*-NH signals reported in this section are consistent with our previous interpretations as follows: the chloride ion interacts with the two *exo*-NH groups; this interaction involves the formation of hydrogen bonds to chloride, and the two chelate rings sterically impede access of the solvent to the *exo*-NH protons.

Effect on the *endo*-NH and Central NH Signals of Cl^- Anion Interaction with the *exo*-NH and Central NH Groups. DMSO-d_6 as the Solvent. The plots of NH signal shift versus the Cl^- concentration (Figures 7−9 and S5 and S6 in the Supporting Information) are revealing. As the Cl^- concentration is increased, particularly beyond the concentration at which the large $\Delta\delta$ of the *exo*-NH signal plateaus, the *endo*-NH signals (and sometimes the central NH signal) shift upfield ($-\Delta\delta$). At higher Cl^- concentration, the shift reverses and the signal may shift downfield slightly ($+\Delta\delta$) from the upfield-shifted position. These $\Delta\delta$'s are not large (< 0.2 ppm and usually < 0.1 ppm), but similar trends were found both in acetonitrile, see below, and in earlier studies.[24] Previously, no attempt was made to explain the small shifts, but it is now clear that these small $\Delta\delta$'s are real and are interpretable.

The $\Delta\delta$ values for the *endo*-NH and central NH signals can be explained by invoking two counteracting factors, one upfield-shifting and the other downfield-shifting. One factor prevails in some cases, and the two factors nearly cancel each other in other cases.

The *downfield-shifting factor* arises from Cl^- hydrogen bonding with the NH group as discussed above. However, both the *endo*-NH and central NH groups are hydrogen-bonded to the solvent and have downfield shifts; thus, the $\Delta\delta$'s are small in comparison to the $\Delta\delta$ observed for the less solvated *exo*-NH groups, which have upfield signals in the absence of Cl^- and exhibit large downfield $\Delta\delta$'s in the presence of Cl^-.

The *upfield-shifting factor* arises from the fact that Cl^- hydrogen bonding with an NH group will result in the release of electron density from the N−H bond into the N−Re and N−C bonds. In the present study, the *exo*-NH bonds of the terminal amines are affected by this hydrogen bonding. In turn, the electron density in the *endo*-NH bonds (and less so in the central NH bond) will increase, causing an upfield shift change ($-\Delta\delta$). This explanation, which we believe is compelling, adds additional evidence that the ion pairing at the *exo*-NH site involves hydrogen bonding. Because interaction of Cl^- at the *exo*-NH site is favorable, this *upfield-shifting factor* is most likely to prevail over the *downfield-shifting factor* at low Cl^- concentration. This reasoning explains the shift changes shown in Figures 7−9 and S5−S9 in the Supporting Information.

For **1** and **6** (Figure 2), the shift patterns of the two *endo*-NH signals in DMSO-d_6 (Figures 7 and 9) are informative. At low Cl^- concentration, the two *endo*-NH signals shift upfield. We believe this behavior is clear evidence for the preferred ion pairing of Cl^- to the *exo*-NH protons, which causes the electron density to increase near the *endo*-NH protons and the consequent upfield shift.

For **1**, as the Cl^- concentration is increased and the ion pairing at the *exo*-NH site is saturated, the Cl^- added to the solution then builds to a sufficient concentration to interact detectably with the central NH, as can be deduced from the reversal of the direction of the shift changes of the central NH signal (Figure 7). This hydrogen bonding of the central NH begins to reverse the direction of the shift change around the plateau Cl^- concentration.

For $[Re(CO)_3(dipn)]^+$, the *endo*-NH $\Delta\delta$ is ~−0.1 ppm. However, for complexes in which the central N has an alkyl group, the *endo*-NH signal upfield shift change is smaller, such as those for **2** ($\Delta\delta \sim -0.03$ ppm; Figure 8), **4** ($\Delta\delta \sim -0.04$ ppm; Figure S5 in the Supporting Information), and **5** ($\Delta\delta \sim -0.07$ ppm; Figure S6 in the Supporting Information). This finding is readily explained by the fact that the central NH hydrogen-bonding site is absent. Thus, after the first anion to interact binds at the preferred *exo*-NH binding site, the next anion to interact with this ion pair necessarily forms a hydrogen bond to the *endo*-NH proton. As a result, the changes in the shift from the two factors (the upfield shift from the electron density changes from *exo*-NH interaction and the downfield shift from *endo*-NH hydrogen bonding) nearly cancel, and only very small *endo*-NH $\Delta\delta$ values are observed (Figures 8 and S5 and S6 in the Supporting Information).

6 in DMSO-d_6 exhibits interesting behavior as the Cl^- concentration increases (Figure 9). The secondary Cl^- anion interaction with the central NH shifts this signal downfield. This is the same shift behavior that we observed previously with $[Re(CO)_3(dien)]^+$.[24] As we suggested above, the extra methylene group of the six-membered rings leads to electron donation to the NH groups. Thus, the central NH is more electron-rich when attached to a six-membered ring. The lower electron density of a five-membered ring of **6** is also indicated by the slight downfield shift of the upfield-shifted five-membered ring *endo*-NH signal (Figure 9). No such $\Delta\delta$ is exhibited by the six-membered ring *endo*-NH signal for **6** (Figure 9).

When Cl^- was added to a 5 mM solution of **7** in DMSO-d_6, only downfield shifting of the NH signal was observed (maximum $\Delta\delta = 0.17$ ppm, light blue full circles; Figure 7). As mentioned above, the NH protons of **7** are directed toward the solvent (Figure 4). Also, our analysis above comparing central NH shifts to the $[Re(CO)_3(tacn)]^+$ NH shift indicates clearly that the NH groups in $[Re(CO)_3(tacn)]^+$ are like the central NH of linear triamines. Thus, the downfield shift observed supports our interpretation that, at high Cl^- concentration, the central NH groups form hydrogen bonds to added Cl^- anion.

For **4**, the Cl^- ion pairing caused a large $\Delta\delta$ for the *exo*-NH (1.2 ppm) signal and a small negative $\Delta\delta$ for the *endo*-NH (−0.04 ppm) signal (Figure S5 in the Supporting Information). This behavior is similar to that of other complexes without the dangling groups, such as **2**. This similarity suggests no synergism involving the dangling NH_3^+ ($\Delta\delta = 0.8$ ppm). Indeed, the protons of the dangling NH_3^+ group of $[Re(CO)_3(trenH)]^{2+}$ cannot come close enough to interact with the Cl^- hydrogen-bonded to the *exo*-NH groups in the 1:1 ion pair. After rotation of the torsion angles using *Chem3D* software, the closest distance between *endo*-NH and NH_3^+ protons is ~3.65 Å. Both protons could interact with a Cl^- anion in an ion pair. However, this type of synergistic ion-pair interaction appears to be unfavorable because neither plateauing of $\Delta\delta$ at low added Cl^- anion concentration nor significant *endo*-NH $\Delta\delta$ values were observed. Similar results were obtained for **5** (Figure S6 in the Supporting Information).

Interaction of Cl^-, Br^-, and I^- Anions with $[Re(CO)_3(dipn)]^+$. Acetonitrile-d_3 as the Solvent. In order to compare the effect of the halide size on ion-pairing interactions with $[Re(CO)_3(dipn)]^+$, the halide titration experiments were performed in acetonitrile-d_3 because we were concerned that the larger halide anions might bind too weakly in DMSO-d_6.

As expected from past studies with Et_4NCl,[24,32] the weakness of the interactions of acetonitrile with the NH group as compared to DMSO facilitates Cl^- interaction with the *exo*-NH groups, leading to larger $\Delta\delta$ and lower Cl^- ion concentration for leveling off of $\Delta\delta$ ($\Delta\delta = 3$ ppm, plateau at ~10 mM Cl^-; Figure S7 in the Supporting Information). As was found previously,[24] the sharpness of the shift changes makes the NMR method for determining ion-pairing equilibrium constants inaccurate.

The above titration was repeated with a "buffering" amount of 50 mM Et_4NPF_6. Aliquots of a stock solution of 150 mM Et_4NCl and 5 mM $[Re(CO)_3(dipn)]^+$ were

(32) Perera, T.; Marzilli, P. A.; Fronczek, F. R.; Marzilli, L. G. *Inorg. Chem.* **2010**, *49*, 2123–2131.

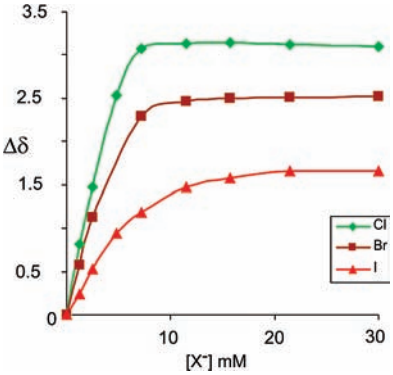

Figure 10. Effect of Cl^-, Br^-, and I^- on $\Delta\delta$ of the *exo*-NH signals of **1** in acetonitrile-d_3 at 25 °C.

added into a 5 mM $[Re(CO)_3(dipn)]^+$/50 mM Et_4NPF_6 solution in acetonitrile-d_3. The $\Delta\delta$ values obtained [Figure S7 (right) in the Supporting Information] were almost identical with those obtained without added PF_6^- [Figure S7 (left) in the Supporting Information].

When the Et_4NBr salt was used, the final $\Delta\delta$ (2.5 ppm) was slightly less than that for Et_4NCl; the plateau occurred at ~10 mM Br^- (Figure S8 in the Supporting Information). A much higher Et_4NI concentration (~15 mM) was required to reach a plateau ($\Delta\delta$ = 1.5 ppm) (Figure S9 in the Supporting Information). The interaction of halide ions with the *exo*-NH groups thus decreases in the order $Cl^- > Br^- > I^-$ (Figure 10).

Of some interest, the two counteracting factors (hydrogen-bonding-induced electron density changes at the proton and anion hydrogen bonding) influencing $\Delta\delta$ of the *endo*-NH signal and the central NH signal in DMSO-d_6 also explain the $\Delta\delta$ of these NH signals in acetonitrile-d_3. In particular, as shown in Figure S9 in the Supporting Information, the *endo*-NH signal of $[Re(CO)_3(dipn)]^+$ in acetonitrile-d_3 shifts upfield rather little ($\Delta\delta$ = −0.1 ppm) with added I^- compared to the effect of Cl^- ($\Delta\delta$ = −0.4 ppm). A small upfield shift could be caused by the downfield-shifting effect of direct I^- interaction with the *endo*-NH signal. However, I^- has a very small direct effect. Thus, the smallness of the upfield shift undoubtedly arises from the weakness of the interaction of I^- with the *endo*-NH group. The interaction of I^- causes very little change in the electron density at the *endo*-NH proton. The results fully support our conclusions above.

Interaction of the Paramagnetic Anion, $[ReBr_6]^{2-}$, with $[Re(CO)_3(dipn)]^+$. When $[Bu_4N]_2[ReBr_6]$ was added to a 5 mM solution of $[Re(CO)_3(dipn)]^+$ in acetonitrile-d_3, upfield shift changes (negative $\Delta\delta$) for the NH signals were observed. At 1.65 mM $[ReBr_6]^{2-}$, $\Delta\delta$ for the *exo*-NH (−3.6 ppm) signal was much greater than that for the *endo*-NH (−1 ppm) signal. However, during titration, the *exo*-NH signal of **1** was often lost under CH_2 multiplets (both from **1** and from $[Bu_4N]^+$ ions) in the ^1H NMR spectral region of 1−3.5 ppm.

We reasoned that by exchanging the NH groups to ND groups to obtain $[Re(CO)_3(dipn\text{-}d_5)]^+$ and by performing ^2H NMR spectroscopy on the sample in a normal solvent (CH_3CN), we should be able to obtain exact $\Delta\delta$ values throughout the titration. Accordingly, ^2H NMR experiments were performed on $[Re(CO)_3(dipn\text{-}d_5)]^+$ (5 mM, 600 μL) in CH_3CN, and upfield $\Delta\delta$ values were noted upon each addition of aliquots of a 30 mM stock solution of $[Bu_4N]_2[ReBr_6]$ containing 5 mM $[Re(CO)_3(dipn\text{-}d_5)]^+$. Figure 11 shows a plot of $\Delta\delta$ versus $[ReBr_6]^{2-}$ concentration. At a final $[ReBr_6]^{2-}$ concentration of 10 mM, no further upfield shift was observed for the *exo*-ND signal, and the maximum $\Delta\delta$ was −6.1 ppm. For the *endo*-ND signal, the maximum $\Delta\delta$ was only ca. −1.8 ppm. For the central ND signal, $\Delta\delta$ was negligible (0.03 ppm). Thus, the greater sensitivity of the *exo*-ND signal of **1** to the large paramagnetic $[ReBr_6]^{2-}$ anion indicates clearly that this anion interacts with the *exo*-ND groups. The NMR data indicate strong interactions, and we estimate the ion-pairing constant to be greater than 1000 M^{-1}. However, accurate constants cannot be obtained. We further note that the large negative $\Delta\delta$ values leave no doubt that $[ReBr_6]^{2-}$ is acting as an outer-sphere paramagnetic shift reagent.

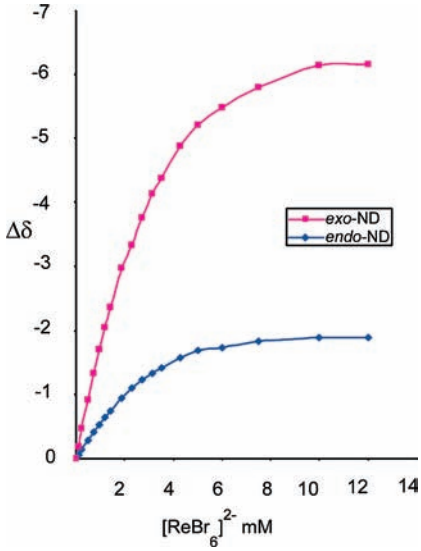

Figure 11. Effect of $[ReBr_6]^{2-}$ on $\Delta\delta$ of the ND signals of $[Re(CO)_3(dipn\text{-}d_5)]PF_6$ in DMSO-d_6 at 25 °C.

A preliminary investigation using $[Re(CO)_3(N,N\text{-}Me_2dipn)]^+$ showed that the *exo*-NH group did not interact strongly with the $[ReBr_6]^{2-}$ anion. This result is consistent with our interpretation of the nature of the anion interactions. Namely, we propose that the anions interact simultaneously with two *exo*-NH groups. Alternatively, the *exo*-NMe group could sterically prevent the anion from closely approaching the *exo*-NH group.

Conclusions. The introduction of a third CH_2 group, changing a dimethylene chain bridging the donor atoms in a five-membered chelate ring to a trimethylene chain, does not significantly alter exposure of the *exo*-NH groups of *fac*-$[Re(CO)_3L]^{n+}$ complexes to the solvent. The *exo*-NH signal is relatively upfield for both five- and six-membered chelate rings. Adding the third CH_2 group affects chiefly the ring conformation and the electron richness of the central NH group anchoring the two chelate rings in *fac*-$[Re(CO)_3L]^{n+}$ complexes.

The six-membered chelate rings favor the chair conformation in both the solid and solution states. Specifically, the most common conformations are designated as being *endo*-C. Thus, COSY data allow unambiguous assignment of the *exo*-NH and *endo*-NH signals, even

when L is a symmetrical ligand. In contrast, the conformational interchange between the λ,λ and δ,δ conformations (or, as we designate the pucker, between the *endo*-C, *exo*-C and *exo*-C,*endo*-C conformations) precludes the use of COSY to assign the NH_2 signals when L is a symmetrical ligand with two five-membered rings. However, at least for L in which there are no dangling groups or in which the dangling group is on the central N, the signals can be assigned by recognizing that the upfield NH signal of the NH_2 group is the *exo*-NH signal.

The electron richness of the central NH group resulting from the third CH_2 group leads to upfield shifts of the NH signal, with the upfield-shifting inductive effect *increasing* along the series: two five-membered rings < one five- and one six-membered ring < two six-membered rings. Consistent with this trend, the interaction of the Cl^- anion with this central NH group (as assessed with ^1H NMR shift changes) *decreases* along this series, as would be expected from the increase in the electron density at the proton. The latter observation reveals the utility of the use of the Cl^- anion in combination with ^1H NMR shift changes to probe the properties of the NH groups of the complexes. This work focuses on *fac*-$[Re(CO)_3L]^{n+}$ complexes of potential radiopharmaceutical utility. However, the anion probe method to assess the solvation around the complexes and the variation in the electron distribution should apply to other types of compounds, including complexes of other metals. Indeed, the $[ReBr_6]^{2-}$ anion appears to be a promising hydrogen-bonding outer-sphere paramagnetic shift reagent, which complements the halide ions used in this study and earlier.[24,32]

The small upfield shifts observed for the *endo*-NH signal support the concept that two *exo*-NH groups simultaneously form hydrogen bonds to the anion in the ion pair. These upfield *endo*-NH shifts are best understood as arising from the increase of the electron density in the *endo*-N−H bond resulting from the interaction of the two *exo*-NH groups with the anion. Larger halide anions form hydrogen bonds in the ion pair, but the interaction is weaker. The alteration of the electronic properties of L decreases with increasing halide size. Ion-pair stability decreases with the halide size. However, the dianionic charge of the large $[ReBr_6]^{2-}$ anion overcomes this instability problem to a large extent, and the increased stability provides another reason that this anion should be explored more fully in the future as an outer-sphere shift reagent.

Acknowledgment. This work was supported by the National Institutes of Health (R37 DK038842). Purchase of the diffractometer was made possible by Grant LEQSF-(1999-2000)-ENH-TR-13, administered by the Louisiana Board of Regents. We thank Prof. Andrew Maverick for discussions and for providing the $[Bu_4N]_2[ReBr_6]$ salt and Dr. Dale Treleaven for his assistance with the ^2H NMR experiments.

Supporting Information Available: Crystallographic data for **1**−**7** in CIF format, NMR signal assignments for **1**−**7**, stacked ^1H NMR spectra of **1**−**6** in DMSO-d_6, selected torsion angles (deg) with figures showing the numbering of selected protons for compounds **1**−**4**, and **6**, $^1H-^1H$ COSY NMR spectra of **1** and **4** in DMSO-d_6, plots showing the dependence of $\Delta\delta$ of the NH signals of **4** and **5** on the Cl^- ion concentration in DMSO-d_6 and of **1** on the Cl^-, Br^-, and I^- ion concentration in acetonitrile-d_3, and ORTEP plots of the cations of **4** and **5**, with the dangling group at N2 deleted for clarity. This material is available free of charge via the Internet at http://pubs.acs.org.